

Neutron Skins and Halo Orbits in the *sd* and *pf* shells

J. Bonnard¹, S. M. Lenzi^{1,2} and A. P. Zuker^{2,3}

¹ *Istituto Nazionale di Fisica Nucleare, Sezione di Padova, 35131 Padova, Italy*

² *Dipartimento di Fisica e Astronomia, Università degli Studi di Padova, I-35131 Padova, Italy*

³ *Université de Strasbourg, IPHC, CNRS, UMR7178, 23 rue du Loess 67037 Strasbourg, France*

(Dated: May 18, 2016)

The strong dependence of Coulomb energies on nuclear radii makes it possible to extract the latter from calculations of the former. The resulting estimates of neutron skins indicate that two mechanisms are involved. The first one—iso-vector monopole polarizability—amounts to noting that when a particle is added to a system it drives the radii of neutrons and protons in different directions, tending to equalize the radii of both fluids independently of the neutron excess. This mechanism is well understood and the Duflo-Zuker (small) neutron skin values derived 14 years ago are consistent with recent measures and estimates. The alternative mechanism involves halo orbits whose huge sizes tend to make the neutron skins larger and have a subtle influence on the radial behavior of *sd* and *pf* shell nuclei. In particular, they account for the sudden rise in the isotope shifts of nuclei beyond $N = 28$ and the near constancy of radii in the $A = 40 - 56$ region. This mechanism, detected here for the first time, is not well understood and may well go beyond Efimov physics usually associated to halo orbits.

Mirror nuclei in which proton and neutron numbers N, Z are interchanged have different energetics due to the isospin breaking interactions (IBI) dominated by the Coulomb force. It affects both the spectra (MED for Mirror Energy Differences) and the ground states (MDE for Mirror Displacement Energies). A prime example of the MED is found in ^{13}Ni where the $1s_{1/2}$ proton orbit is depressed by about 750 keV with respect of its neutron analogue in ^{13}C . This behavior is referred to as Thomas-Ehrman shift (TES) because it was first studied via R-matrix theories by J. Ehrman [1] and R. G. Thomas [2] who also considered the pair ^{17}F - ^{17}O .

The *s* orbits are the essential ingredients of halo physics [3] and have a decisive influence in the spectroscopy of nuclei at $A = 16 \pm 1$ [4, 5], which will be shown to extend to higher masses, including the *pf* shell because of the halo nature of the *p* orbits.

The TES can be viewed as an overbinding of orbits—with respect to naive expectations—because their large radii reduce the Coulomb repulsion. For the binding energies, the naive assumption is that a closed shell core is unperturbed by the addition of a particle. The MDE would then be due to the core Coulomb field acting on the extra proton. The result is often a severe underestimate, as in $A = 41$: the Nolen-Schiffer anomaly (NSA) [6] illustrated in Table I. While the TES is due to a proton radius larger than expected for the extra particle, the NSA may be thought to demand the opposite *i.e.*, a reduction of the radius of the added particle but this is ruled out experimentally [7].

Though Shlomo had noticed that equalizing the total neutron and proton radii would eliminate the anomaly [9] it took some time before this basically sound idea gained traction: Hartree-Fock (HF) calculations routinely predicted proton radii in agreement with experiment and substantially larger neutron radii [10], though experimental evidence did not support the latter [11, 12]. Then it was shown that good proton radii were compatible with

TABLE I. Displacement energies between the ground state of $T = 1/2$ mirror nuclei of mass A defined as $\text{MDE} = E_J(Z > N) - E_J(Z < N)$. Experimental, full IBI, Coulomb (C) and schematic Coulomb (Eq. (1), sC) contributions are given in MeV. No core $0\hbar\omega$ calculation with $V_{\text{low-}k}$ form [8] of the N3LO [27] potential with cutoff $\lambda = 2.0 \text{ fm}^{-1}$.

A	$\hbar\omega$	J^π	MDE_{exp}	MDE_{IBI}	MDE_C	MDE_{sC}
15	14.67	$1/2^-$	3.537	3.574	3.474	3.624
17	13.38	$5/2^+$	3.543	3.388	3.377	3.514
39	10.89	$3/2^+$	7.307	7.120	6.970	7.212
41	10.61	$7/2^-$	7.278	6.683	6.679	6.675

a variety of neutron radii [13, 14] and calculations appeared in which the NSA was almost absent [15]. The NSA does not seem to have attracted much attention lately but neutron radii are a very hot subject whose connection with displacement energies—hitherto somewhat neglected—is worth examining. It follows by noting that isospin conservation implies that the proton rms radius $\rho_{\pi>} = \sqrt{\langle r_{\pi>}^2 \rangle}$ of a nucleus with $Z > N$ equals the neutron rms radius of its mirror, $\rho_{\nu<}$ with $Z < N$. Assuming a schematic Coulomb contribution of the form $C_{Zx} = 0.67Z(Z-1)/\rho_x$ we have (disregarding other IBI terms)

$$\text{MDE} = C_{Z+1\pi>} - C_{Z\pi<} = C_{Z+1\nu<} - C_{Z\pi<} \quad (1)$$

Therefore, if we know, say, $\text{MDE}(^{17}\text{F}-^{17}\text{O})$ and $\rho_{\pi<}$, the proton radius of ^{17}O , we also know its neutron radius $\rho_{\nu<}$. This simple idea lead to a general estimate of the neutron skins by Duflo and Zuker (DZ) [16]. They started by fitting the proton mean square radii to experiment through ($t = N - Z$)

$$\sqrt{\langle r_\pi^2 \rangle} = \rho_\pi = A^{1/3} \left(\rho_0 - \frac{\zeta}{2} \frac{t}{A^{4/3}} - \frac{v}{2} \left(\frac{t}{A} \right)^2 \right) e^{(g/A)} \quad (2)$$

$$+ \lambda [z(D_\pi - z)/D_\pi^2 \times n(D_\nu - n)/D_\nu^2] A^{-1/3} \quad (3)$$

where n , z are the number of active particles between the EI magic numbers [17, Sec. IC] at N , $Z = 6, 14, 28, 50, \dots$; $D_x = 8, 14, 22, \dots$ are the corresponding degeneracies. By fitting known radii for $A \leq 60$ one obtains rms deviations of about 42 mf for a 4 parameter fit with $\lambda = 0$ reduced to about 18 mf when varying λ . (Including all known radii the rms deviation goes down, with little change in the parameters). In principle the neutron skin (in fm)

$$\Delta r_{\nu\pi} = \rho_\nu - \rho_\pi = \frac{\zeta t}{A} e^{g/A}, \quad (4)$$

could be expected to come out of the fit. However, fixing ζ to values between 0.4 and 1.2 did not alter the quality of the fit. A useful reminder that the neutron radii are independent of the proton ones. Hence, the authors resorted to Eq. (1) using a form of the Coulomb potential close to the exact one for oscillator orbits. We adopt the set $g = 0.985$, $\rho_0 = 0.944$, $\lambda = 5.562$, $v = 0.368$, $\zeta = 0.8$, $\text{rmsd} = 0.0176$. All units in fm except g . With these values of g and ζ Eq. (4) yields the estimates of Table II where they are seen to agree with numbers of diverse origin: a recent measure [18], estimates based on comparison with electric dipole polarizability α_D [19] and an “*ab initio*” calculation [20]. It should be noted (stressed) that the

TABLE II. Comparing $\Delta r_{\nu\pi}$ from Eq. (4) with estimates (ests) [19, 20] and measure (exp) [18] (fm).

	^{48}Ca	^{68}Ni	^{120}Sn	^{208}Pb	^{128}Pb
Eq. (4)	0.14	0.14	0.13	0.17	0.17
ests-exp	0.135(15)	0.17(2)	0.14(2)	0.16(3)	0.15(3)
ref.	[20]	[19]	[19]	[19]	[18]

results of Eq. (4) also square nicely with those obtained from two other sources analyzed in [23]: they are very close to the Gogny D1S force [21] and not far from those of Sly4 [22]—which gives slightly bigger skins. It appears that a general mechanism, that we sketch next, is at play. Think of a model space in which an extra particle (dot in Fig 1 taken to be a neutron) associated to number n and isospin t polarizes the system by inducing particle-hole jumps from the closed core of particles h to the open shells of particles p $2\hbar\omega$ above. While H_0 represents isoscalar monopole polarizability, responsible for an overall increase in radius, its isovector counterpart, H_1 takes care of a differential contraction-dilation of the fluids. The model could be termed the “degree zero” of the mean field [24]:

$$H_0 = \varepsilon S_0 + v_0 n(S_+ + S_-), \quad \varepsilon = \frac{1}{2}(\varepsilon_p - \varepsilon_h), \quad (5)$$

$$S_0 = \hat{n}_p - \hat{n}_h, \quad S_+ = a_p^+ a_h + b_p^+ b_h + hc,$$

$$H_1 = \varepsilon S_0 + v_1(t_- U_+ + t_+ U_- + \frac{1}{2} t_0 U_0), \quad (6)$$

$$U_0 = a_p^+ a_h - b_p^+ b_h + a_h^+ a_p - b_h^+ b_p,$$

$$U_+ = a_p^+ b_h + a_h^+ b_p, \quad U_- = b_p^+ a_h + b_h^+ a_p.$$

A unitary (HF) transformation solves exactly H_0 but only approximately H_1 because the term in $t_- U_+ + t_+ U_-$ demands a more refined treatment, ignored here. The results can be visualized in Fig. 1. The shaded area corresponds to the unperturbed Hamiltonian bounded by a parabola, while the heavy lines represent parabolic segments with $\hbar\omega_\nu > \hbar\omega_\pi$, the situation in which the NSA disappears as the radii tend to equalize *i.e.*, reduce the neutron skin with respect to the $\hbar\omega_\nu = \hbar\omega_\pi$ value. The sign of v_1 determines whether radii equalize or move apart. Within this elementary mean field approach all orbits behave in the same way. A more refined approach would allow different polarizabilities for different orbits. Moreover, the model ignores threshold effects *i.e.*, coupling to the continuum that could play an important role.

Nonetheless the model has the advantage of suggesting the computational strategy that generalizes the DZ approach. We shall work in $0\hbar\omega$ no-core spaces with $V_{\text{low-}k}$ [8] precision potentials: AV18 [25], CDB [26], and N3LO [27] which produce almost indistinguishable results according to our checks. They incorporate effects not treated in DZ (such as electromagnetic spin-orbit coupling) are fully IBI and will make it possible to do configuration mixing. Saturation is treated in the standard shell model way by fixing $\hbar\omega$ at a value consistent with the observed radius. It is here that Fig. 1 comes in: For each nucleus, calculations are done for a different $\hbar\omega$ for neutrons and protons: $\hbar\omega_\pi$ is known through Eqs. (2,3,7) for $N > Z$ (and hence $\hbar\omega_\nu$ for $N < Z$). Then $\hbar\omega_\nu$ for $N > Z$ and $\hbar\omega_\pi$ for $N < Z$ follow from ζ treated as a free parameter to reproduce the experimental MDE or MED. To relate $\hbar\omega_\pi$ to the radii we adapt from [28, Eq.(2.157)] Eq. (7), where the sum runs over occupied proton orbits in oscillator shells of principal quantum number p , and a similar expression for neutrons, leading asymptotically to Eq. (8).

$$\hbar\omega_\pi = \frac{41.47}{\langle r_\pi^2 \rangle} \sum_i z_i(p_i + 3/2)/Z, \quad (7)$$

$$\frac{\hbar\omega_\pi}{(2Z)^{1/3}} = \frac{35.59}{\langle r_\pi^2 \rangle}; \quad \frac{\hbar\omega_\nu}{(2N)^{1/3}} = \frac{35.59}{\langle r_\nu^2 \rangle}. \quad (8)$$

The form of $\hbar\omega$ as a function of A is obtained through a

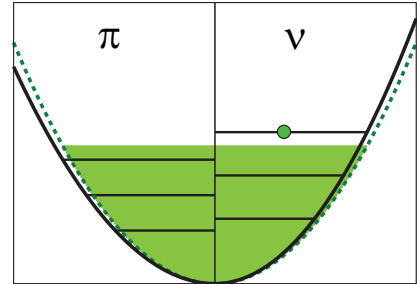


FIG. 1. (color online) Illustrating the solution of Eq. (6). Explained in text.

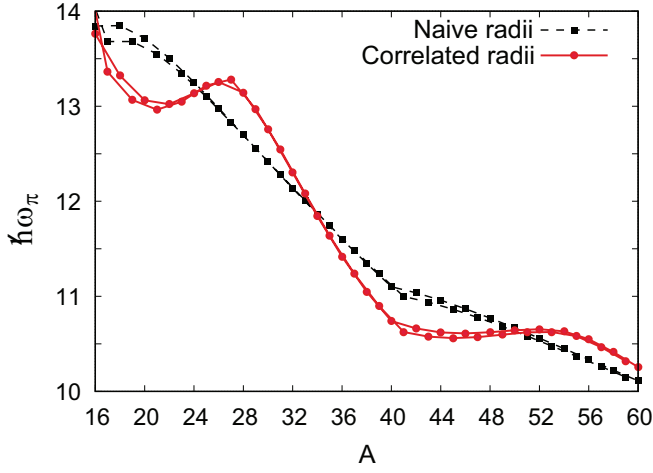


FIG. 2. (color online) Values of $\hbar\omega_\pi$ (MeV) for $T = 0$ and $1/2$ extracted from Eq. (7) using ρ_π from Eqs. (2,3) with parameters $g = 0.985$, $\rho_0 = 0.944$, $\lambda = 5.562$, $v = 0.368$, $\zeta = 0.8$, for the correlated radii and $\lambda = 0$. for naive radii. All units in fm except g .

term by term (nucleus by nucleus) evaluation of Eq. (7). Two variants are chosen: $\lambda = 0$ in Eqs. (2) (the naive fit) and $\lambda \neq 0$ —the correlated fit—leading to the interesting pattern in Fig 2. Its meaning may not be evident at first, but clarification comes in Fig. 3—showing the isotope shifts of the K and Ca isotopes, including recent measures [30, 31]—which make it clear that Duflo’s λ term has a deep physical grounding: The abrupt raise of radii after $A = 47$ *i.e.*, the $N = 28$ is an open problem [30, 31], so far only qualitatively explained by relativistic mean field calculations [32]. Fig. 3 suggests a very simple solution: the raise is due to the filling of *huge* $p_{3/2}$ orbits. As the filling occurs for neutron orbits, and the shift measures the behavior of proton orbits, isovector polarizability must be at work here: if one fluid increases in size, the other fluid must follow suit. The operation of the λ term does not depend on ζ , which may take any value, but must be fairly constant. To learn some more about the nature of $s_{1/2}$ and $p_{3/2}$ which seem (are) responsible for the elegant undulating patterns in Fig. 2, we examine the single particle and single hole states built on ^{16}O and ^{40}Ca .

Results are given in Table III and Fig. 4. The values of ζ have been adjusted so as to obtain the observed energies. In the figure, the calculated ζ and $\Delta r_{\nu\pi}$ are compared with those obtained under the $\hbar\omega_\nu = \hbar\omega_\pi$ (naive shell model) assumption, expected to produce too large skins. However, because of the pronounced shell effects exhibited in the plots, for the hole states *i.e.*, $A = 15$ and 39 the skins remain moderate or small. A few comments:

$A = 15$. Independently of the ζ values, $\hbar\omega_\nu < \hbar\omega_\pi$ rules out an isovector polarization mechanism. As there is no simple argument to treat these orbits as “halo”, we prefer to leave the question open.

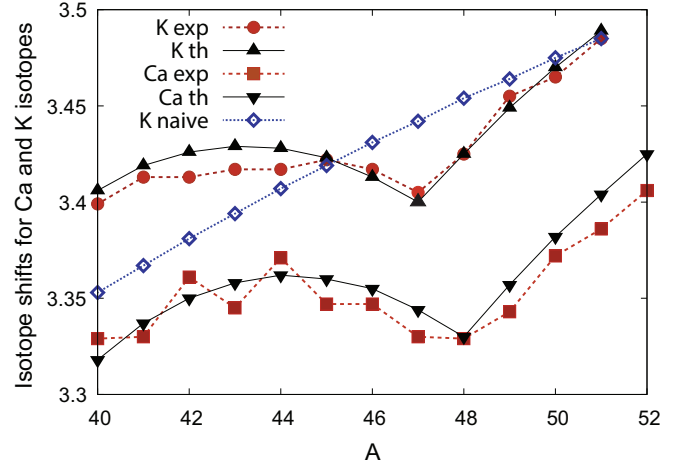


FIG. 3. (color online) Radii ρ_π in fm from isotope shifts in the K and Ca isotopes [29] incorporating recent measures [30, 31](label exp) compared with estimates from Eqs.(2,3) (parameters as in Fig. 2, label naive is for $\lambda = 0$). The correlated numbers (label th) have been shifted down by 30 mf, to restore translation invariance and allow for experimental uncertainties in the extraction of radii ρ_π from $\delta\langle r_\pi^2 \rangle$ isotope shifts. For clarity the K and Ca values are shifted by ± 55 mf respectively

TABLE III. MDE and MED ΔE for $T = 1/2$ mirror nuclei of mass A , $\hbar\omega_{\nu,\pi}$ in MeV and the corresponding skin parameters and radii in fm. Note that the radii correspond to the $N > Z$ nuclei, they are interchanged for the mirror partners. Experimental and calculated ΔE values coincide by construction. Interaction N3LO [27] with cutoff $\Lambda = 2\text{fm}^{-1}$.

A	J^π	ΔE	$\hbar\omega_\nu$	$\hbar\omega_\pi$	ζ	$\Delta r_{\nu\pi}$	r_π	r_ν
15	$1/2^-$	3.537	14.55	14.62	0.358	0.025	2.507	2.532
	$3/2^-$	3.389	14.39	14.66	0.609	0.043	2.503	2.547
17	$5/2^+$	3.543	13.62	13.38	0.906	0.056	2.641	2.697
	$1/2^+$	3.167	12.86	13.51	2.367	0.147	2.628	2.776
39	$3/2^+$	7.307	10.97	10.91	0.258	0.007	3.361	3.368
	$1/2^+$	7.253	10.90	10.89	0.523	0.014	3.365	3.379
41	$7/2^-$	7.278	10.78	10.63	0.610	0.015	3.422	3.437
	$3/2^-$	7.052	10.61	10.59	1.513	0.038	3.427	3.465
	$1/2^-$	7.129	10.61	10.59	1.482	0.037	3.428	3.465
	$5/2^-$	7.351	10.75	10.61	0.702	0.018	3.424	3.442
	$5/2^-$	7.338	10.75	10.61	0.725	0.018	3.427	3.442

$A = 17$. A reasonable value of ζ solves the NSA for $d_{5/2}$. The $s_{1/2}$ orbit is truly large: its rms radius is about 1.2 fm larger than its $d_{5/2}$ counterpart. No doubt about its halo nature.

$A = 39$. Here we find that $s_{1/2}$ is no longer gigantic, but large enough to keep some memory of its halo status.

$A = 41$. Most interesting. NSA is solved for $f_{7/2}$ via a reasonable ζ very close to what is demanded by the lowest observed pair of $f_{5/2}$ candidates which have only a fraction of the spectroscopic strength. Both $p_{3/2}$ and $p_{1/2}$ are accommodated by the same ζ and have pronounced

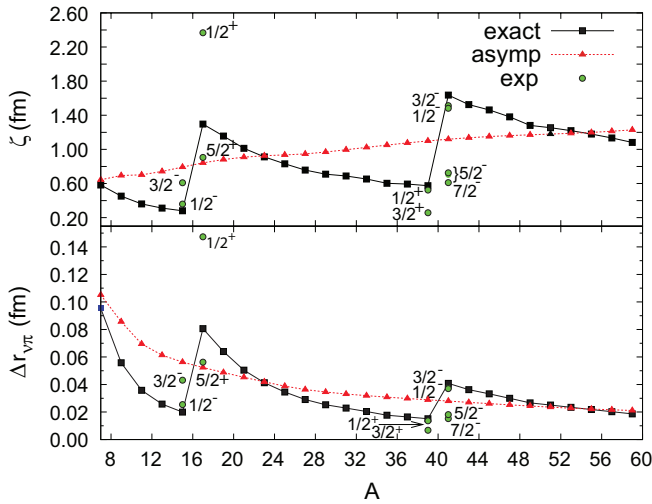


FIG. 4. (color online) Values of ζ and $\Delta r_{v\pi}$ from Table III (dots labeled exp) compared with those obtained for $\hbar\omega_\nu = \hbar\omega_\pi$ from Eqs. (7) (labeled exact) and (8) (labeled asympt).

halo nature. Their rms radii exceed those of the f orbits by some 0.7 fm. Interestingly, orbits of the same l have the same behavior.

Old problems come back under new guises: the NSA as neutron skins, the TES as halo orbits associated to subtle shell effects detected in isotope shifts.

Neutron skins are difficult to measure experimentally.

Recent progress has been made [18] and their connection with the isovector dipole polarizability α_D have led to reliable estimates [19]. Theoretically the problem is much simpler. It is subsumed by isovector monopole polarizability [24], or for Skyrme type functionals by control of the symmetry energy [13, 14]. As noted after Table II, several calculations appear to reproduce skins well.

Halo orbits are another matter: no existing calculation [30, 31] explains the observed isotope shifts as done in Fig. 3. We have interpreted the result as due to an increase in size of a p orbit. We have also learned from Table III and Fig. 4 that $s_{1/2}$ and $p_{3/2}$ are so huge that they could be viewed as halo orbits in $A = 17$ and 41, but their influence extends well beyond. We have also learned that at $A = 39$, $s_{1/2}$ is no longer huge. We expect to learn much about its evolution through full MED and MDE configuration mixing calculations now under way.

We close by proposing an alternative to the use of Eq. (3) to represent shell effects:

$$\langle r_\pi^2 \rangle = \frac{41.47}{\hbar\omega_\pi} \sum_i z_i (p_i + 3/2 + \delta_i) / Z \quad (9)$$

where $\hbar\omega_\pi$ is now the “naive” estimate using Eq. (2) alone and the δ_i corrections to the oscillator values replace the λ term. Eq. (9) could be useful in interpreting the structure of isotope shifts as reflecting orbital occupancies associated to given orbital radii.

-
- [1] J. Ehrman, Phys. Rev. **81**, 412 (1951).
 - [2] R. G. Thomas, Phys. Rev. **88**, 1109 (1952).
 - [3] I. Tanihata, H. Savajols and R. Kanungo, Progress in Particle and Nuclear Physics **68**, 215 (2013).
 - [4] K. Ogawa, H. Nakada, S. Hino, and R. Motegi: Phys. Lett. **B464**, 157 (1999).
 - [5] L. V. Grigorenko, T. A. Golubkova, and M. V. Zhukov, Phys. Rev C **91**, 024325 (2015).
 - [6] J. A. Nolen and J. P. Schiffer, Phys. Lett. **B29**, 396 (1968), J. A. Nolen and J. P. Schiffer, Ann., Rev. Nucl. Sci. **19**, 471 (1969).
 - [7] S. Platchkov *et al.*, Phys. Rev. Lett. **61**, 1465 (1988).
 - [8] S. K. Bogner, T. T. S. Kuo, and A. Schwenk, Phys. Rept. **386**, 1 (2003).
 - [9] S. Shlomo, PhD Thesis Weizmann Institute 73/21 ph, 1973 unpublished.
 - [10] S. Shlomo, Rep. Prog. Phys. **41**, 958 (1977).
 - [11] S. Shlomo and E. Friedman, Phys. Rev. Lett. **39**, 1180 (1977).
 - [12] G. K. Varma and L. Zamick, Nucl. Phys. **A306**, 343 (1978).
 - [13] J. M. G. Gómez and J. Martorell, Nucl. Phys. **A410**, 475 (1983).
 - [14] B. A. Brown Phys. Rev. Lett. **85**, 5296 (2000).
 - [15] B. K. Agrawal, Tapas Sil, S. K. Samaddar, J. N. De and S. Shlomo, Phys. Rev. C **64**, 024305 (2001).
 - [16] J. Duflo and A. P. Zuker, Phys. Rev. C **66**, 051304(R) (2002).
 - [17] E. Caurier, G. Martínez-Pinedo, F. Nowacki, A. Poves, and A. P. Zuker, Rev. Mod. Phys. **77**, 427 (2005).
 - [18] C. M. Tarbert *et al.*, Phys. Rev. Lett. **112**, 242502 (2014).
 - [19] X. Roca-Maza *et al.*, Phys. Rev. C **92**, 064304 (2015).
 - [20] G. Hagen *et al.*, Nat. Phys. **12**, 186 (2016)
 - [21] J. F. Berger, M. Girod and D. Gogny, Comput. Phys. Commun. **63**, 365 (1991).
 - [22] E. Chabanat *et al.*, Nucl. Phys. **A635**, 231 (1998).
 - [23] M. Warda *et al.* Phys. Rev. C **81**, 054309 (2010).
 - [24] A. P. Zuker Czech. J. Phys. B **25**, 311 (1975).
 - [25] R. B. Wiringa and V. G. J. Stoks and R. Schiavilla, Phys. Rev. C **51**, 38 (1995).
 - [26] R. Machleidt and F. Sammarruca and Y. Song, Phys. Rev. C **53**, R1483 (1996).
 - [27] D. R. Entem and R. Machleidt, Phys. Lett. **B524**, 502 (2002) Physical Review C **68**, 041001 (2003).
 - [28] A. Bohr and B. Motelsson, Nuclear Structure, vol. I, Benjamin, 1969, New York.
 - [29] I. Angeli, K. P. Marinova, At. Dat. Nucl. Data Tables **99**, 69 (2013).
 - [30] K. Kreim *et al.*, Phys. Lett. **B731**, 97 (2014).
 - [31] R. F. García Ruiz *et al.*, Nature Physics, online, 8 Feb. 2016, DOI: 10.1038/NPHYS3645
 - [32] G.A. Lalazissis, T. Niksić, D. Vretenar, P. Ring, Phys.

Rev. C **71**, 024312 (2005).